Dynamics of a Bottlenecked $S = 1$ Spin System*

W. J. Brya
Sandia Laboratories, Albuquerque, New Mexico 87115
(Received 2 October 1970)

The dynamics of an inhomogeneously broadened $S=1$ system strongly coupled to a bottlenecked lattice are analyzed in the context of the usual rate-equation formalism. The center of the $\Delta M_S = \pm 1$ resonance is characterized by an equally spaced three-level system, while the wings of the resonance are viewed as an almost equally spaced level system in which resonant phonons are noninteracting. Calculations of phonon heating under rf saturation of the spin transitions show the phonon linewidths to be noticeably less than the EPR bandwidth; conservation conditions which relate the various phonon excitations are also obtained and extended to a general multilevel system. Determinations of the normal unbottlenecked spin-relaxation rate and the intrinsic phonon decay times are possible at early times in the decay to equilibrium, while an analytic expression for the final asymptotic decay rate of the coupled system is obtained in the limit of a large phonon lifetime . Numerical solutions to the rate equations at early times are also presented and discussed in terms of the strong competition between resonant phonons for the spin-excitation energy.

I. INTRODUCTION

At low temperatures, spin-lattice relaxation may occur through a direct phonon process which transfers energy to the crystal lattice at the spin-resonance frequency. If the spin-phonon coupling is strong and the thermalizing process for the resonant phonons is slow, the usual assumption that the lattice is in thermal equilibrium may break down, and phonon heating can occur. Such a situation, now commonly known as a phonon bottleneck, modifies the spin-system decay, and the relaxation is governed largely by the rate at which excess phonons can be dissipated.

The possibility of such a phonon bottleneck was first recognized by Van Vleck[1] in the early 1940's. Since then, a wealth of theoretical and experimental information on the phenomenon has been accumulated.[2-14] The early experimental data have dealt primarily with the spin decay characteristics, from which the phonon behavior can often be inferred. Only recently have more direct measurements of the phonon-system properties been reported.[7,9-13]

Since a large part of the experimental work has been directed toward $S=\frac{1}{2}$ systems, much of the theoretical effort[2-5,8] has also followed this trend. However, recent experimental studies[7,10,14] in a number of $S=1$ systems, for which the theory is sparse, have yielded considerable information on the bottleneck problem; in addition, very recent measurements[15] in one such system (MgO: Ni^{2+}) provide the most complete study to date of the phonon-system properties.

It is the purpose of this paper, therefore, to extend the existing theory to the more general $S=1$ system. Section II examines the spin-phonon behavior for the case of equal spin-level spacings, as would occur in the ideal $S=1$ configuration, while Sec. III is concerned with a nearly equally spaced system in which all phonons are uncoupled. In Sec. IV, we examine our results in terms of a typical inhomogeneously broadened $S=1$ resonance line and further extend a number of our conclusions to the general multilevel spin system.

II. EQUALLY SPACED THREE-LEVEL SYSTEM

We consider initially the three-level configuration depicted in Fig. 1, which is characteristic of the ground state of an $S=1$ spin system in a pure octahedral environment. An external Zeeman field splits the levels equally by an energy $\delta = \hbar\omega_1$ with their respective populations n_i. The spins are assumed coupled to the lattice only through the emission and absorption of resonant phonons of energies δ and $2\delta = \hbar\omega_2$ (we neglect Raman and Orbach relaxation via an excited state); the resonant phonon excitations are $p_i = (e^{\hbar\omega_i/kT_{\rm eff}^{(i)}} - 1)^{-1}$, where $T_{\rm eff}^{(i)}$ is an effective phonon temperature which may or may not be equal to the ambient (bath) temperature T.

The simplest model for a study of the dynamics of a strongly coupled spin-phonon system is based

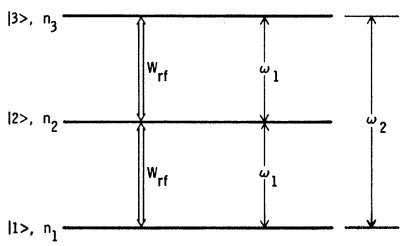

FIG. 1. Energy-level diagram for $S=1$ spin system with equal spacing $\hbar\omega_1$ of states $|i\rangle$ (with populations n_i). W_{rf} denotes rf field saturation at frequency ω_1.

on rate equations for the level populations n_i and the phonon excitations p_i, an approach which has yielded quite reasonable results for the simpler two-level system.[2,3] In the usual manner, the rate equations for the level populations can be written

$$\frac{dn_1}{dt} = -(w_{12}+w_{13})n_1 + w_{21}n_2 + w_{31}n_3 - W_{rf}(n_1 - n_2),$$

$$\frac{dn_3}{dt} = -(w_{31}+w_{32})n_3 + w_{13}n_1 + w_{23}n_2 - W_{rf}(n_3 - n_2),$$

where w_{ij} is the single-phonon transition probability from level $|i\rangle$ to level $|j\rangle$,[16] and $n_1+n_2+n_3 = N$ is the total number of spins. The last term in each equation represents the effect of any rf field-induced transition probability W_{rf} at frequency ω_1 on the level populations. Following the formalism of Faughnan and Strandberg,[2] we assume a linear-loss mechanism for the phonons, such that the phonon lifetime is τ_i in the absence of any interaction with the spins, and write for the phonon rate equations

$$\frac{dp_1}{dt} = [\rho(\omega_1)d\omega_1]^{-1}(w_{32}n_3 - w_{23}n_2 + w_{21}n_2 - w_{12}n_1) - \tau_1^{-1}(p_1 - p_1^0),$$

$$\frac{dp_2}{dt} = [\rho(\omega_2)d\omega_2]^{-1}(w_{31}n_3 - w_{13}n_1) - \tau_2^{-1}(p_2 - p_2^0),$$

where $\rho(\omega_i)d\omega_i$ is the number of lattice modes in the frequency interval $d\omega_i$ which interact with the ions, and the superscript denotes a thermal-equilibrium value. We define new normalized variables

$$N_i = 3n_i/N, \quad Y_i = (p_i - p_i^0)/\sigma_i(p_i^0 + \tfrac{1}{2}), \tag{1}$$

where

$$\sigma_1 = 2NK_1\tau_1/3(p_1^0+\tfrac{1}{2})\rho(\omega_1)\,d\omega_1,$$

$$\sigma_2 = NK_2\tau_2/3(p_2^0+\tfrac{1}{2})\rho(\omega_2)\,d\omega_2 \tag{2}$$

are the "bottlenecking factors" for phonons of energies δ and 2δ, and the K_i are the spontaneous emission rates for direct relaxation at frequencies ω_i. After some rearrangement, the rate equations become

$$\begin{aligned}\frac{dN_1}{dt} = -K_1\{&(2p_1^0+1+k_{21}p_2^0)N_1 + [p_1^0+1-k_{21}(p_2^0+1)]N_3 \\ &+\sigma_1(p_1^0+\tfrac{1}{2})(2N_1+N_3-3)Y_1 \\ &+k_{21}\sigma_2(p_2^0+\tfrac{1}{2})(N_1-N_3)Y_2 \\ &-3(p_1^0+1)\} - W_{rf}(2N_1+N_3-3),\end{aligned} \tag{3}$$

$$\begin{aligned}\frac{dN_3}{dt} = -K_1\{&(p_1^0-k_{21}p_2^0)N_1 + [2p_1^0+1+k_{21}(p_2^0+1)]N_3 \\ &+\sigma_1(p_1^0+\tfrac{1}{2})(N_1+2N_3-3)Y_1 \\ &-k_{21}\sigma_2(p_2^0+\tfrac{1}{2})(N_1-N_3)Y_2 \\ &-3p_1^0\} - W_{rf}(N_1+2N_3-3),\end{aligned}$$

$$\begin{aligned}\frac{dY_1}{dt} = -(2\tau_1)^{-1}\{&(p_1^0+1)N_1 - p_1^0N_3 - 3 \\ &+[\sigma_1(p_1^0+\tfrac{1}{2})(N_1-N_3)+2]Y_1\},\end{aligned}$$

$$\begin{aligned}\frac{dY_2}{dt} = -\tau_2^{-1}\{&p_2^0N_1 - (p_2^0+1)N_3 \\ &+[\sigma_2(p_2^0+\tfrac{1}{2})(N_1-N_3)+1]Y_2\},\end{aligned} \tag{4}$$

with $k_{ij} = K_i/K_j$. In Eqs. (3), the terms in Y_1 and Y_2 indicate the effects of the excess phonons on the spin decay rates, while normal unbottlenecked relaxation is represented by the remaining terms (with $W_{rf} \equiv 0$). As in the two-level system, the σ_i represent the ratio of power transferred from spins to phonons to the power transferred from phonons to bath. For $\sigma_i \ll 1$ one obtains the usual unbottlenecked relaxation profiles, while for $\sigma_i \gtrsim 1$ one expects marked deviations from exponential behavior. With τ_i and $d\omega_i$ independent of frequency and temperature, and a Debye density of phonon states, a non-Kramers system will show $\sigma_i \propto \omega_i^2/Td\omega_i$ for small $\hbar\omega_i/kT$. The bottleneck will therefore be enhanced at high Zeeman frequencies and low bath temperatures.

The above rate equations are nonlinear and as such are not readily soluble; however, in certain instances one can obtain useful and informative solutions. We begin by considering a saturated spin system and its subsequent decay to equilibrium.

At saturation, we have $dN_i/dt = dY_i/dt \equiv 0$, with $N_i \equiv 1$. From Eqs. (4) we find $Y_i \equiv 1$ which, for $kT_{eff}^{(i)} \geq kT > \hbar\omega_i$, is rewritten to obtain

$$T_{eff}^{(i)} \simeq (\sigma_i + 1)T. \tag{5}$$

Thus, even for steady-state spin saturation, the phonon temperature is limited to the finite result of Eq. (5) which can be reasonably estimated using Eq. (2). As shown earlier, $\sigma_i \propto T^{-1}$, and Eq. (5) becomes $T_{eff}^{(i)} = \beta_i + T$, with β_i temperature independent. For large bottlenecking, the phonon excitation is therefore large and constant at low bath temperatures but approaches equilibrium with increasing temperature. We also note that the phonon temperature given by Eq. (5) can be specialized to any given phonon of frequency ω_i (with specific polarization and propagation direction) out of the totality of phonons ω_i, provided one uses the appropriate quantities in the evaluation of σ_i. This is not the case after removal of the rf field, when the various monoenergetic phonons can compete unequally for the spin energy during the decay to equilibrium.

The complete decay profiles of the spin and phonon excitations are only obtainable using numerical techniques. We see from Eqs. (3), however, that at the start of the decay the spin relaxation is given by the usual unbottlenecked rates, irrespective of the phonon excitations; this results from the cancellation of induced emission and absorption at saturation. The phonon excitations, meanwhile, begin their decays with zero slope – the phonon excitations cannot change until the spin excitation is altered.

The behavior of the N_i and Y_i can also be determined near the end of the decay where $N_i \to N_i^0$ and $Y_i \to 0$. By replacing the bilinear terms in $N_i Y_j$ by $N_i^0 Y_j$, we obtain a new set of four coupled linear equations. Although these are analytically soluble in principle, one can also determine approximate solutions which are quite accurate in the limiting case $\sigma_i \gg 1$. The exponential decay rates are readily obtained using a straightforward matrix diagonalization procedure: If one constructs the matrix A_{jk} of the coefficients of the variables N_i and Y_i, the eigenvalues λ_j of this matrix are the required rates. In general, for $\sigma_i \gg 1$ and $\tau_i \ll 1$ (a valid assumption in almost all cases), one finds that the coefficients of the variables Y_i in the equations for dY_i/dt are typically orders of magnitude greater than any of the other coefficients. This indicates that the matrix is almost partially diagonal and these larger coefficients are, to a very good approximation, required eigenvalues. With these eigenvalues (rates) determined, one can now solve for the remaining rates. This is done by equating coefficients of the parameter λ of the characteristic equation of our original matrix $|A_{ij} - \lambda\delta_{ij}| = 0$ to the coefficients of the characteristic equation for the actual eigenvalue λ_i, $|(\lambda_i - \lambda)\delta_{ij}| = 0$; the still unknown λ_i can then be determined to any order in the bottlenecking factors σ_i.

Using this technique we have solved the linearized forms of Eqs. (3) and (4), to lowest order in σ_i, and have obtained the following decay rates when $\sigma_i \gg 1$:

$$\lambda_1 = -(2\tau_1)^{-1}[\sigma_1(p_1^0+\tfrac{1}{2})(N_1^0 - N_3^0) + 2],$$

$$\lambda_2 = -\tau_2^{-1}[\sigma_2(p_2^0+\tfrac{1}{2})(N_1^0 - N_3^0) + 1],$$

$$\lambda_3 = -3K_1[p_1^0 + (1 - N_3^0)/(N_1^0 - N_3^0)], \tag{6}$$

$$\lambda_4 = \frac{-2K_1}{3[p_1^0(N_1^0 - N_3^0) + 1 - N_3^0]}\left(\frac{3(p_1^0)^2 + 3p_1^0 + 1}{\sigma_1(p_1^0+\tfrac{1}{2})}\right.$$

$$\left. + k_{21}\frac{3p_1^0 p_2^0 - 1 + 3(p_1^0 + p_2^0 + 1)[(1 - N_3^0)/(N_1^0 - N_3^0)]}{\sigma_2(p_2^0+\tfrac{1}{2})}\right).$$

The first three rates are effective in establishing internal equilibrium within the coupled spin-phonon system; since this is not applicable in the present case, we will defer further discussion of them until later. The fourth and smallest term λ_4 represents the decay rate of the coupled spin-phonon system to the thermal bath and characterizes the long-time relaxation rates normally measured in spin-lattice relaxation studies. This rather cumbersome expression can be greatly simplified by considering several limiting cases. For $\hbar\omega_1 \ll kT$, one finds

$$\lambda_4 \simeq -\left(\frac{kT}{\hbar\omega_1}\right)^2\left(\frac{K_1}{\sigma_1(p_1^0+\tfrac{1}{2})} + \frac{K_2}{2\sigma_2(p_2^0+\tfrac{1}{2})}\right),$$

which further simplifies to $\lambda_4 \propto \omega_1^0 T^2$. Thus, the relaxation rate increases quadratically with the bath temperatures and is independent of the level splittings, just as in the two-level system. With $\hbar\omega_1 \gg kT$, one obtains

$$\lambda_4 \simeq -\tfrac{2}{3}K_1/\sigma_1(p_1^0+\tfrac{1}{2}).$$

Now we have $\lambda_4 \propto \omega_1^2 T^0$, so that the rate is temperature independent but varies quadratically as the level splittings. In all cases, λ_4 is inversely proportional to the spin concentration and shows a dependence on sample size when τ_i is determined by boundary-scattering processes.

It appears from the foregoing expressions that λ_4 is independent of K_i, the spontaneous-emission rates. This is illusory since σ_i also involves other parameters which are contained in K_i, e.g., $\rho(\omega_i)$. However, with the exception of $d\omega_i$ the interaction bandwidth, these parameters are characteristic of the lattice, not the spin system. For large σ_i, one therefore expects similar ions doped into a given lattice host to show the same long-time behavior, other things being equal. This is not unexpected since, for a large bottleneck, the relaxation of a tightly coupled spin-phonon system should be governed by the loss mechanism for the excess phonons.

In Fig. 2, we show results of numerical solutions to Eqs. (3) and (4) for early times. The values of the parameters chosen are typical of a number of systems (e.g., MgO:Ni^{2+}). The decay profiles for the spin excitations are not depicted since they

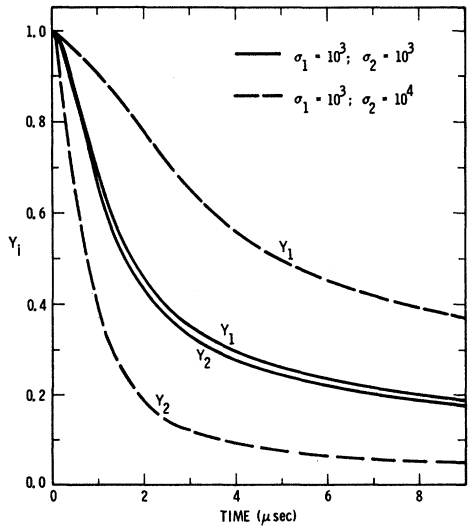

FIG. 2. Phonon-relaxation curves following saturation of all spin transitions depicted in Fig. 1 for $T = 2$ °K, $\omega_1 = 25.6$ GHz, $K_1 = 100$ sec^{-1}, $k_{21} = 10$, $\tau_i = 1$ μsec, $\sigma_1 = 10^3$, and $\sigma_2 = 10^3$, 10^4. Spin excitations show negligible change over given time interval.

experience little change over the given time interval: The spins begin their relaxation with the unbottlenecked decay time which increases monotonically to the asymptotic time. The decays of the phonon excitations, however, show a markedly different behavior: The decays begin with zero slope as required, quickly speed up over a short period of time, and then slow down and proceed to equilibrium, over a much longer time.[17] This is in sharp contrast to the expected exponential decays one would obtain if the spin system were not present. One finds that increases in either K_1, k_{21}, σ_1, or σ_2 (while holding the other parameters fixed) cause the phonon decay to turn over sooner at the onset and to drop more rapidly at the early times. The initial decay, however, cannot proceed at a greater rate than the intrinsic phonon decay rate τ_i^{-1}; only a decrease in τ_i can further shorten this time. The final return to equilibrium occurs at the rate λ_4, as has been shown earlier. However, even after an appreciable time into the decay, when the phonon excitation has dropped to a fraction of its initial value, the decay is still proceeding at a rate much greater than the final asymptotic value (for our examples, the decay times several milliseconds into the relaxation are still in the msec regime). Thus, one has to rely on spin-lattice relaxation measurements to determine the asymptotic rate λ_4; the main interest in the phonon decays occurs only at the very early times, where a determination of τ_i is possible.

We now consider the relaxation behavior for the case where the spin system is initially placed in a negative temperature state (inversion of populations) and the phonon excitations are left at their equilibrium values. Experimentally, this is accomplished using either the adiabatic rapid-passage[18] or 180°-pulse technique.[19] In particular, we examine the case of total spin inversion where the initial spin temperature is $-T$, the negative of the ambient temperature.

Initially, the spins begin their decays with the usual unbottlenecked rates, while the phonon build-ups begin with small but nonzero values. It is not immediately obvious that later in the decay one can once again obtain the unbottlenecked rates. As evidenced by Eqs. (3), this requires that all the spin transitions reach saturation simultaneously, a feat which may not be possible for all choices of our parameters; numerical solutions to the equations are required to answer this question. We also note from Eqs. (4) that, for $N_1 = N_3$ and $Y_i \gg N_i$, the phonon relaxation proceeds at the intrinsic rate τ_i^{-1}. One therefore has the capability of determining this rate by monitoring the phonon decay as the $\Delta M_S = 2$ spin transition passes through saturation. For very long times, the coupled spin-phonon system will again decay at the asymptotic rate λ_4 given by Eq. (6).

Numerical solutions to the rate equations for the case $\sigma_1 = \sigma_2$ are presented in Fig. 3, where decay profiles for the various spin transitions are depicted. ΔN_{ij} signifies the quantity $(N_j - N_i)/(N_i^0 - N_j^0)$, a normalized level population differential which represents the strength of the usual EPR resonance transition between levels $|i\rangle$ and $|j\rangle$. $\Delta N_{ij} = -1$ corresponds to the thermal-equilibrium resonance; $\Delta N_{ij} = 0$ and 1 signify saturation and total inversion of the transition, respectively. Values of $\Delta N_{ij} > 1$ indicate an inverted-state resonance greater than the equilibrium resonance. One notes the pronounced nonexponential decays: The relaxation begins slowly at the unbottlenecked rate, speeds up quickly and then slows down once again as it proceeds to equilibrium at the asymptotic rate λ_4. This is very similar to the behavior obtained for the two-level system. Of particular note, however, is the profile of ΔN_{12}. In this instance, the transition starts in an emissive state, quickly passes through saturation to an absorptive configuration, returns more slowly to its saturation state, and then proceeds to its final equilibrium value. This behavior arises from the competition between the $\Delta M_S = 1$ and $\Delta M_S = 2$ spin transitions and will be discussed in greater detail when we consider the $\sigma_2 > \sigma_1$ case. We might note

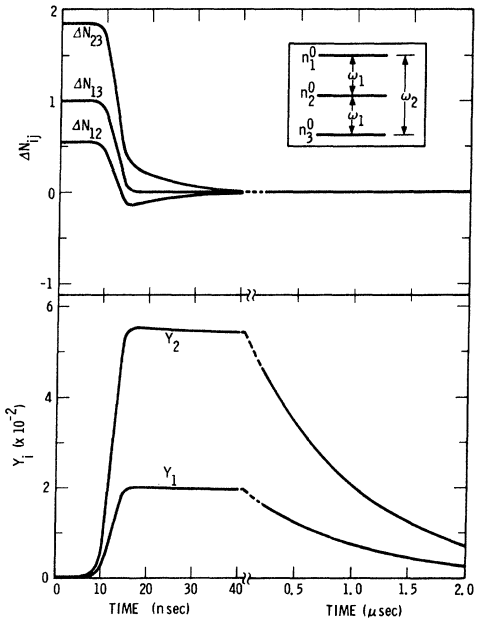

FIG. 3. Spin-system and phonon-relaxation curves determined from Eqs. (3) and (4) following spin inversion. Insert shows initial spin configuration; n_i^0 signifies population of level $|i\rangle$ at thermal equilibrium. Parameters are the same as for Fig. 2 except $\sigma_1 = \sigma_2 = 10^3$. Note break in time scale.

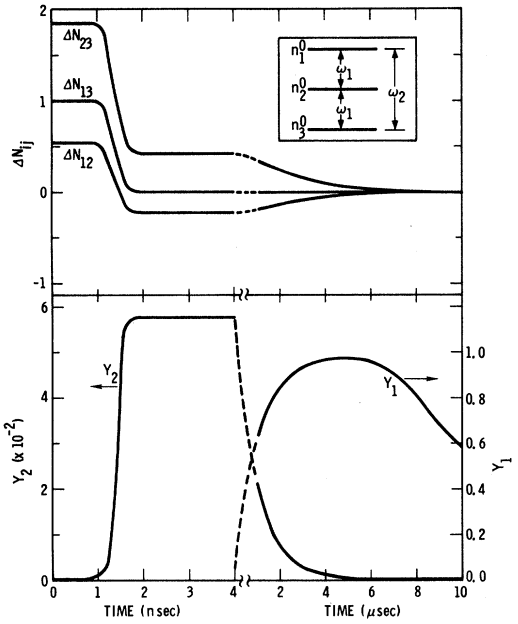

FIG. 4. Relaxation profiles for spin and phonon systems after spin inversion shown in insert. The parameters of Fig. 2 are applicable except $\sigma_1 = 10^3$, $\sigma_2 = 10^4$.

here that, at some given time, all transitions do pass through saturation simultaneously and the unbottlenecked decay rates can be determined.

Also shown in Fig. 3 are the responses of the phonons to the spin-system perturbation. The phonons increase slowly at first and then quickly build up as the spin transitions drop to saturation (this occurs with rates of the order of λ_1 and λ_2).[20] After peaking, the phonons begin a slow return to equilibrium which, however, is initially faster than the spin-system decay; as expected, the decay rates at saturation are just the intrinsic τ_i^{-1}. The phonons peak at essentially the same time with $Y_2 > Y_1$, although both are large. Variations of the other system parameters cause only quantitative differences in the decays with the exception of k_{21}; a reduction of k_{21} causes the dip in the ΔN_{12} relaxation to be gradually removed.

Figure 4 illustrates the relaxation for the case $\sigma_2 \gg \sigma_1$. The ΔN_{13} transition behaves very similarly to that of the preceding example, while ΔN_{12} and ΔN_{23} show more interesting behavior. ΔN_{12} has the same dip below saturation as the previous case; however, it lasts for a much greater length of time and maintains a constant limiting value. ΔN_{23} shows a rapid relaxation to less spin inversion, which it holds for a considerable time, and then more slowly approaches saturation. This behavior is readily understood when one notes that the initial fast decay of the spins is associated with relaxation via ω_2 phonons; the N_1 and N_3 populations quickly come into internal equilibrium with $N_1 = N_3 = \frac{1}{2}(N_1^0 + N_3^0)$, while N_2 remains unchanged. Over a longer time the tightly coupled N_1 and N_3 relax to N_2 through the generation of ω_1 phonons and all the transitions approach their saturation values. This is further pointed up in the phonon profiles of Fig. 4. Y_2 rises rapidly to its large peak value and then decays away, beginning with the intrinsic rate τ_2^{-1}. Y_1, on the other hand, builds up very slowly to a small peak value $Y_1 \sim 1$; here one does not have the opportunity to determine τ_1 as $Y_1 \lesssim N_i$. Although not observable from our figure, the various spin transitions do not pass through saturation simultaneously; however, the deviations are small enough that decays measured at "saturation" will probably be good estimates of the unbottlenecked rates.

Numerical decay profiles for the case $\sigma_1 \gg \sigma_2$ have also been obtained but are not shown here. Their behavior is qualitatively similar to that of the case $\sigma_2 \gg \sigma_1$ with a few exceptions: In this instance, Y_1 peaks considerably ahead of Y_2 in time and its intensity is typically several orders of magnitude greater. The peak of Y_2 occurs quite late in time (analogous to the behavior of Y_1 in the previous case) and is limited to $Y_2 \sim 1$. Neither ΔN_{12} nor any of the other transitions shows a dip or plateau in their decay and all transitions pass through saturation at the same time. For $\Delta N_{13} = 0$, the decay of Y_1 proceeds at the rate τ_1^{-1}, while τ_2 is undetermined.

We should point out at this time that an experimental determination of the behavior of ΔN_{12} or ΔN_{23} using resonance techniques is unfortunately not possible. Because of the equal level splittings, any attempt to monitor either quantity separately leads to a measurement of ΔN_{13}; and, as we have noted earlier, the ΔN_{13} transition decays to equilibrium without displaying any of the unique behavior of the other ΔN_{ij}.[21]

III. NEARLY EQUALLY SPACED THREE-LEVEL SYSTEM

We now consider a three-level spin system which possesses nearly equal level splittings, a scheme which is also characteristic of an $S = 1$ system but one in which a small axial-field component (arising, say, from local lattice strains) distorts the pure octahedral environment of the spin. An external Zeeman field yields the level splittings of energies $\hbar\omega_i$ depicted in Fig. 5. We assume a total of N spins: By allowing for an axial distortion of either sign, one obtains two subsystems each of population $\frac{1}{2}N$ with level populations n_i and m_i, respectively. We further assume that the only coupling between the systems arises through the resonant phonons with excitations p_i, which themselves are assumed noninteracting, and allow for an rf field of transition probability W_{rf} at the frequency ω_1 as before.

Using the previous formalism one can obtain rate equations for the quantities n_i, m_i, and p_i. We define normalized variables

$$N_i = 2n_i/N, \quad M_i = 2m_i/N,$$
$$Y_i = 4(p_i - p_i^0)/3\sigma_i(p_i^0 + \tfrac{1}{2}) \quad \text{for } i = 1, 3, \tag{7}$$
$$Y_2 = 2(p_2 - p_2^0)/3\sigma_2(p_2^0 + \tfrac{1}{2}),$$

where σ_1 and σ_2 are defined by Eq. (2) and

$$\sigma_3 = 2NK_3\tau_3/3(p_3^0 + \tfrac{1}{2})\,\rho(\omega_3)\,d\omega_3 . \tag{8}$$

The applicable rate equations then become

$$\begin{aligned}
\frac{dN_1}{dt} = &-K_1\{[p_1^0 + k_{21}(2p_2^0 + 1)]N_1 \\
&+ [-(p_1^0 + 1) + k_{21}(p_2^0 + 1)]N_2 \\
&+ \tfrac{3}{4}\sigma_1(p_1^0 + \tfrac{1}{2})(N_1 - N_2)Y_1 \\
&+ \tfrac{3}{2}k_{21}\sigma_2(p_2^0 + \tfrac{1}{2})(2N_1 + N_2 - 1)Y_2 \\
&- k_{21}(p_2^0 + 1)\} - W_{rf}(N_1 - N_2), \\
\frac{dN_2}{dt} = &-K_1\{[-p_1^0 + k_{31}(p_3^0 + 1)]N_1 \\
&+ [(p_1^0 + 1) + k_{31}(2p_3^0 + 1)]N_2 \\
&+ \tfrac{3}{4}\sigma_1(p_1^0 + \tfrac{1}{2})(N_2 - N_1)Y_1 \\
&+ \tfrac{3}{4}k_{31}\sigma_3(p_3^0 + \tfrac{1}{2})(N_1 + 2N_2 - 1)Y_3 \\
&- k_{31}(p_3^0 + 1)\} - W_{rf}(N_2 - N_1), \\
\frac{dM_2}{dt} = &-K_1\{[p_1^0 + k_{31}(2p_3^0 + 1)]M_2 + [-(p_1^0 + 1) + k_{31}p_3^0]M_3 \\
&+ \tfrac{3}{4}\sigma_1(p_1^0 + \tfrac{1}{2})(M_2 - M_3)Y_1 \\
&+ \tfrac{3}{4}k_{31}\sigma_3(p_3^0 + \tfrac{1}{2})(2M_2 + M_3 - 1)Y_3 \\
&- k_{31}p_3^0\} - W_{rf}(M_2 - M_3),
\end{aligned} \tag{9}$$

$$\begin{aligned}
\frac{dM_3}{dt} = &-K_1\{(-p_1^0 + k_{21}p_2^0)M_2 \\
&+ [(p_1^0 + 1) + k_{21}(2p_2^0 + 1)]M_3 \\
&+ \tfrac{3}{4}\sigma_1(p_1^0 + \tfrac{1}{2})(M_3 - M_2)Y_1 \\
&+ \tfrac{3}{2}k_{21}\sigma_2(p_2^0 + \tfrac{1}{2})(M_2 + 2M_3 - 1)Y_2 \\
&- k_{21}p_2^0\} - W_{rf}(M_3 - M_2), \\
\frac{dY_1}{dt} = &\,\tau_1^{-1}\{-p_1^0(N_1 + M_2) + (p_1^0 + 1)(N_2 + M_3) \\
&+ [\tfrac{3}{4}\sigma_1(p_1^0 + \tfrac{1}{2})(N_2 - N_1 + M_3 - M_2) - 1]Y_1\}, \\
\frac{dY_2}{dt} = &\,\tau_2^{-1}\{-(2p_2^0 + 1)(N_1 - M_3) - (p_2^0 + 1)N_2 + p_2^0M_2 + 1 \\
&+ [\tfrac{3}{2}\sigma_2(p_2^0 + \tfrac{1}{2})(2M_3 + M_2 - 2N_1 - N_2) - 1]Y_2\}, \\
\frac{dY_3}{dt} = &\,\tau_3^{-1}\{-(p_3^0 + 1)N_1 - (2p_3^0 + 1)(N_2 - M_2) + p_3^0M_3 + 1 \\
&+ [\tfrac{3}{4}\sigma_3(p_3^0 + \tfrac{1}{2})(2M_2 + M_3 - N_1 - 2N_2) - 1]Y_3\}.
\end{aligned}$$

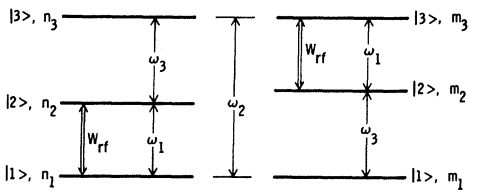

FIG. 5. Energy-level diagram for $S=1$ spin system with nearly equal spacing of states; the subsystems n_i and m_i are described in the text. Level splittings are greatly exaggerated; $\omega_1 \simeq \omega_3$. rf field saturation occurs only at frequency ω_1.

For steady-state saturation ($W_{rf} \to \infty$) of the ΔN_{12} and ΔM_{23} transitions, Eqs. (9) $\equiv 0$, with $N_1 = N_2$, $M_2 = M_3$. The relations $dN_i/dt = dM_i/dt \equiv 0$ are of little interest, because of the existence of the rf field term. These are therefore replaced by the expressions $d(N_1 + N_2)/dt = d(M_2 + M_3)/dt \equiv 0$. The equations for saturation then become

$$\begin{aligned}
\frac{d(N_1 + N_2)}{dt} = 0 = &-K_1\{[k_{21}(3p_2^0 + 2) + k_{31}(3p_3^0 + 2)]N_1 \\
&+ \tfrac{3}{2}k_{21}\sigma_2(p_2^0 + \tfrac{1}{2})(3N_1 - 1)Y_2 \\
&+ \tfrac{3}{4}k_{31}\sigma_3(p_3^0 + \tfrac{1}{2})(3N_1 - 1)Y_3 \\
&- k_{21}(p_2^0 + 1) - k_{31}(p_3^0 + 1)\}, \\
\frac{d(M_2 + M_3)}{dt} = 0 = &-K_1\{[k_{21}(3p_2^0 + 1) + k_{31}(3p_3^0 + 1)]M_2 \\
&+ \tfrac{3}{2}k_{21}\sigma_2(p_2^0 + \tfrac{1}{2})(3M_2 - 1)Y_2 \\
&+ \tfrac{3}{4}k_{31}\sigma_3(p_3^0 + \tfrac{1}{2})(3M_2 - 1)Y_3 \\
&- k_{21}p_2^0 - k_{31}p_3^0\},
\end{aligned} \tag{10}$$

$$\begin{aligned}
\frac{dY_1}{dt} = 0 = &\,\tau_1^{-1}(N_1 + M_2 - Y_1), \\
\frac{dY_2}{dt} = 0 = &\,\tau_2^{-1}\{-(3p_2^0 + 2)N_1 + (3p_2^0 + 1)M_2 + 1 \\
&+ [\tfrac{9}{2}\sigma_2(p_2^0 + \tfrac{1}{2})(M_2 - N_1) - 1]Y_2\}, \\
\frac{dY_3}{dt} = 0 = &\,\tau_3^{-1}\{-(3p_3^0 + 2)N_1 + (3p_3^0 + 1)M_2 + 1 \\
&+ [\tfrac{9}{4}\sigma_3(p_3^0 + \tfrac{1}{2})(M_2 - N_1) - 1]Y_3\}.
\end{aligned}$$

With $dY_1/dt = 0$, we have $Y_1 = N_1 + M_2$. Using Eq. (7) and assuming $kT_{eff}^{(1)} > kT > \hbar\omega_1$, this yields

$$T_{eff}^{(1)} \simeq [\tfrac{3}{4}\sigma_1(N_1 + M_2) + 1]\,T. \tag{11a}$$

The solutions of Eq. (10) for N_1 and M_2 are not readily available, as we shall show shortly. It is easily shown, however, that the largest value for $N_1 + M_2 = \frac{2}{3}$ is obtained when all transitions are saturated; for the general case, Eq. (11a) becomes

$$T_{eff}^{(1)} \lesssim (\tfrac{1}{2}\sigma_1 + 1)\,T. \tag{11b}$$

With strong bottlenecking, then, the heating of the

resonant phonons ω_1 is at least a factor of 2 less than the heating obtained when the levels are equally spaced.

The determination of the saturation values for the other variables involves the solution of a quartic equation which is further reduced to a cubic. Except for a few limiting cases, the solution is best accomplished using numerical techniques and yields only one physically realizable situation. Typically, we have $N_1 + M_2 < \frac{2}{3}$ and $Y_2 > 0 > Y_3$, with both $Y_i \sim 0$. The reduction of the quartic equation to a cubic is of particular interest as it yields the relation

$$Y_2/Y_3 = -k_{32} = -K_3/K_2 . \tag{12a}$$

Rewriting Eq. (12a) using the results of Eqs. (2), (7), and (8), one finds

$$\tau_2^{-1}(p_2 - p_2^0)\,\rho(\omega_2)\,d\omega_2 = -\tau_3^{-1}(p_3 - p_3^0)\,\rho(\omega_3)\,d\omega_3 , \tag{12b}$$

which directly relates the phonon excitations p_2 and p_3. Equation (12b) represents a necessary phonon conservation condition: The rate at which ω_2 phonons are lost to the bath must equal the rate at which ω_3 phonons are removed from the bath. In retrospect, this is not unexpected with the system undergoing cw saturation at frequency ω_1. Since all level populations and phonon excitations are unchanging, transitions into and out of N_3 and M_1 must be compensated by the only available energy source for phonons, the bath. A similar relationship involving the ω_1 phonons is unnecessary since they are fed directly from an external source, the saturating rf field.

When the rf field is removed, the phonon excitations begin their decays with zero slope; the spin transitions, however, do not begin their relaxation with the unbottlenecked rates, as that requires equal populations in all levels. For very long times the asymptotic decay rates are obtained from the linearized forms of Eq. (9) using our approximation techniques. These rates show little deviation from those obtained for the system with equally spaced levels: One obtains three large rates of the form λ_1 and λ_2 in Eq. (6), two intermediate rates comparable to λ_3, and two small rates comparable to, though often slightly larger than, λ_4.

Early-time decay profiles with $k_{31} = 1$ and $\sigma_1 = \sigma_3$, as would be expected for an almost equally spaced $S = 1$ system, were also obtained. Once again the spin relaxation is characterized by a rate $\sim \lambda_4$. The Y_1 phonon decay is qualitatively similar to that for the equally spaced system although the initial fast decay is more subdued; changes in σ_2 have little effect on Y_1. Y_2 and Y_3 show no obvious nonexponential behavior and return to equilibrium at the asymptotic rate $\sim \lambda_4$.

Following a perturbation which inverts all or part of the spin system, but leaves the phonons at the ambient temperature, the spins begin their decays with the normal unbottlenecked rates. Later, one can again determine the normal rates providing all transitions ΔN_{ij}, ΔM_{ij} pass through saturation simultaneously. The intrinsic rate τ_i^{-1} for the phonons Y_i is more readily obtained since one only requires that the spin transitions of energy $\hbar\omega_i$ pass through saturation simultaneously and $Y_i \gg$ all N_i, M_i.

If one initially inverts a single transition ω_i, as is easily done using either the 180°-pulse or adiabatic rapid-passage technique, the results of Fig. 6 are obtained. Choosing $\Delta N(\omega_i)$, $\Delta M(\omega_i)$ to represent the normalized population differentials of the two subsystems at the ω_i transition frequency, we plot the quantity

$$\Delta L_i = -[\Delta N(\omega_i) + \Delta M(\omega_i)]/[\Delta N^0(\omega_i) + \Delta M^0(\omega_i)] ,$$

which is proportional to the usual ESR resonance strength for the ω_i transition; for example, for the transition at frequency ω_1, we have

$$\Delta L_1 = (N_2 - N_1 + M_3 - M_2)/(N_1^0 - N_2^0 + M_2^0 - M_3^0) .$$

For all choices of parameters the perturbed transition ω_1 shows typical bottleneck behavior. However, the other transitions never do pass through saturation and the normal relaxation rates are undetermined. The phonons Y_1 show a large peak early in time while Y_2, $Y_3 \sim 0$ with $Y_2 > 0 > Y_3$. In all cases τ_1 is obtained when the ΔL_1 transition

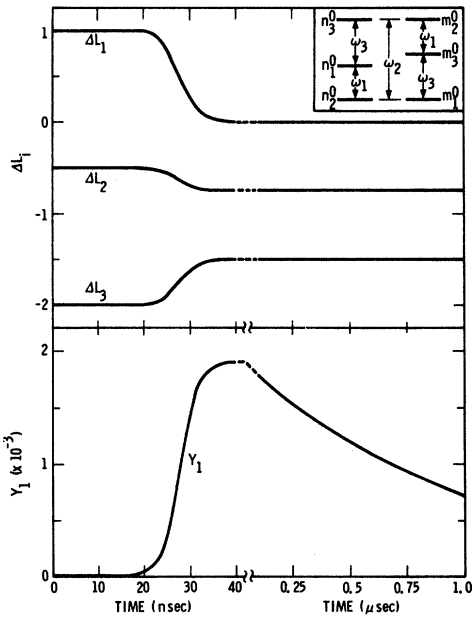

FIG. 6. Spin- and phonon-relaxation curves obtained from Eqs. (9) following inversion of ω_1 transitions (see insert). Parameters same as for Fig. 2 except $\omega_1 = \omega_3 = 25.6$ GHz, $k_{31} = 1$, $\sigma_1 = \sigma_3 = 10^3$, and $\sigma_2 = 10^4$. Curves for Y_2 and Y_3 show little change and are not presented.

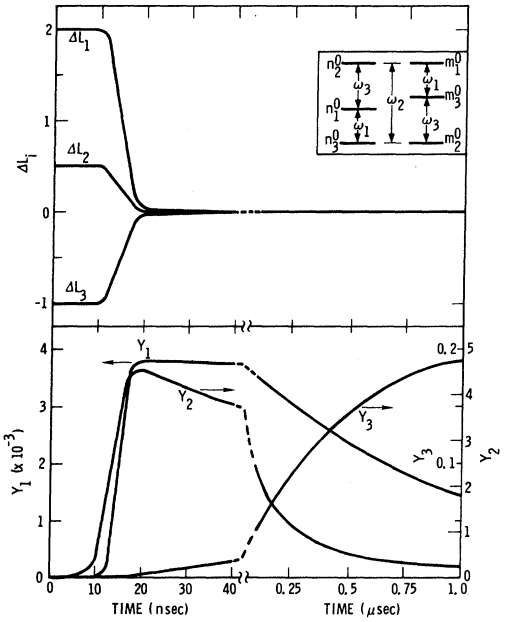

FIG. 7. Relaxation profiles for spin and phonon systems following sequential inversion of ω_3 and ω_1 transitions as shown in insert. Parameters are the same as for Figs. 2 and 6 except $\sigma_1 = 10^3$.

passes through saturation.

The decay profiles of greatest interest are obtained for the initial spin configuration shown in the insert of Fig. 7. Using the rapid-passage scheme, the transitions ω_3 and ω_1 are inverted sequentially in time and the spin decay is monitored at one frequency ω_i. For equal σ_i, all the ΔL_i transitions show the usual initial fast decay: ΔL_1 and ΔL_2 drop rapidly from the inverted state to saturation; ΔL_3, on the other hand, starts with its equilibrium value and rises rapidly to saturation. At very long times, ΔL_3 and the other ΔL_i return again to equilibrium at the asymptotic rate. As seen from the phonon curves, the initial spin behavior is associated with rapid increases in Y_1 and Y_2, while Y_3 increases slowly over a much longer time. All the ΔL_i essentially pass through saturation together but, even though the ω_3 phonons do not participate in the fast decay, this does not necessarily prevent a determination of the normal relaxation rates. With the ω_1 and ω_2 transitions initially inverted, their rapid decay to saturation and the attendant buildups in Y_1 and Y_2 might, in certain instances, produce equal populations in all the spin levels.[22] This would be expected to occur for $\sigma_1 \sim \sigma_2$ and one could then obtain the unbottlenecked rates. In general, however, the decay at saturation will not be the desired normal rate with equal σ_i. The decay of Y_1 after peaking occurs with the rate τ_1^{-1}, while the τ_i for the other Y_i are unavailable.

For the same initial spin configuration, the relaxation characteristics for $\sigma_1 \gg \sigma_2$ are very similar to the preceding example; the only qualitative difference is a Y_2 behavior comparable to that of Y_3. The unbottlenecked rates are undetermined and Y_1 decays with its intrinsic rate.

The unique profiles of Fig. 8 occur for the case $\sigma_2 \gg \sigma_1$. On their approach to saturation, the ΔL_1 and ΔL_2 transitions display two rapid decays which coincide with the generation of large numbers of phonons at the frequencies ω_1 and ω_2. Particularly noteworthy is the ΔL_3 decay with its many changes in spin temperature before it finally returns to equilibrium. The spin decay rates at saturation are uninformative since the sequential generation of phonons at ω_2 and ω_1 cannot produce equal level populations. The behavior of Y_2 is also quite interesting. After its initial increase, Y_2 begins its decay to equilibrium at the rate τ_2^{-1}. As Y_1 increases, however, the Y_2 excitation very quickly drops to near equilibrium and remains there. Y_1 reaches its maximum value and then decays away with τ_1. The rapid decay of Y_2 has its basis in the competition between the ω_1 and ω_2 transitions: The initial large excitation of Y_2 arises when the bottleneck drives the ω_2 transitions to saturation. However, as Y_1 increases and the ω_1 transitions are driven to saturation, the ω_2 transitions are thereby forced toward their equilibrium values. Since a large bottleneck factor favors a transition in a saturated condition, ω_2 phonons are reabsorbed to keep the uppermost levels at the same popula-

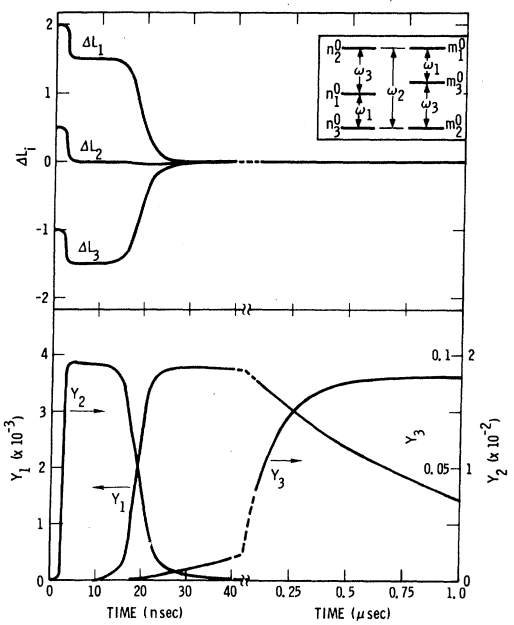

FIG. 8. Spin-phonon decay curves obtained from Eqs. (9); initial spin configuration shown in insert. Properties same as Fig. 7 with $\sigma_1 = \sigma_3 = 10^3$ and $\sigma_2 = 10^4$.

tions as the lowest levels and Y_2 drops. A further indication of this competition is aptly demonstrated in the decay curve for ΔL_3 which shows a slight dip toward equilibrium at the time when Y_1 and Y_2 are exchanging excitations.

IV. DISCUSSION

In a number of $S=1$ spin systems, the EPR line attributed to $\Delta M_S = \pm 1$ transitions is inhomogeneously broadened by random lattice strains. As a result, only at the center of the resonance is the system describable by the equally spaced level scheme. In the wings of the resonance, the $\Delta M_S = 1$ transitions are well resolved and the situation is more aptly characterized by the nearly equally spaced configuration just described.[23]

With cw saturation at or sufficiently removed from line center, the phonon heating is readily obtained using the general expressions Eqs. (5) and (11). Since the excitation at line center will be at least twice as large as that experienced in the wings of the line, even with equal numbers of spins present, a profile of phonon heating, as a function of that portion of the EPR line undergoing saturation, will display a line shape of width noticeably less than the EPR bandwidth. By comparison, a bottlenecked two-level system with an inhomogeneous resonance will show a phonon profile quite similar to the EPR line.

The situation is considerably different for those phonons generated by $\Delta M_S = \pm 2$ spin transitions. With saturation of the $\Delta M_S = 1$ transitions at energy δ, significant phonon heating at 2δ is only possible at line center where the exchange of energy between spin levels is relatively easy. As a result, the phonon bandwidth will be significantly less than either the EPR or δ-phonon linewidth.

In truth, the phonon properties will be further influenced by other processes not considered here: spin diffusion, internal cross-relaxation,[24] spin transition and phonon-excitation overlap, double-quantum transitions,[25,26] etc. Generally these will lead to a lessening of the phonon excitation and further broadening of the phonon bandwidth. Quantitative estimates as to the importance of these effects are not readily available; however, direct measurements of the phonon profiles obtained with saturation of selected portions of the resonance should show the significance of such processes in any particular case.

As noted earlier, the expressions for the phonon excitation can be easily specialized to any given phonon providing the bottleneck factor σ is appropriately evaluated. This feature should be of particular interest in a material of high crystal symmetry where strong selection rules govern the spin-lattice coupling in the presence of an applied magnetic field. Studies of phonon heating as a function of magnetic field orientation and phonon polarization and propagation should provide further useful information about the spin-phonon coupling formalism in the $S=1$ system and other more general systems.

The phonon conservation condition of Eq. (12b) obtained for the nearly equally spaced spin system also has far-reaching implications. For a multilevel spin system in which one or more transitions are undergoing rf saturation, the excitations of resonant phonons of frequencies different from the rf field frequency are uniquely interrelated through expressions of the type Eq. (12b). In fact, these relationships are valid for any degree of rf saturation provided only that the coupled spin-phonon system is in a steady-state configuration; the degree of saturation only influences the absolute excitations of the phonons and not their relative values.

As indicated in our calculations, further information on the spin-phonon–system parameters is obtained when the rf field is removed. Spin-lattice relaxation measurements at the center of the resonance show the decay to begin with the normal unbottlenecked relaxation rate, a feature which is typical of any multilevel spin system provided all transitions are initially saturated; measurements of the phonon decays at early times yield the intrinsic phonon-relaxation rates when the bottleneck factors are large and could prove useful in studies of phonon-lifetime phenomena. At long times the coupled system returns to equilibrium at the asymptotic rate derived earlier, a rate which is characterized by an inverse dependence on the number of spins, a linear relationship to sample size when boundary scattering is dominant, and quite often by a distinctive T^2 temperature dependence.

The relaxation behavior following an initial spin inversion yields similar quantitative results, often with increased experimental accuracy; determinations of the normal relaxation rate, intrinsic phonon decay times, and the asymptotic decay rate are usually possible at some period in the return to equilibrium. In addition, the qualitative behavior of the decays for various choices of the bottleneck factors and the initial spin configuration are also of some interest, since the rather distinctive profiles often provide added information as to the relative importance of the different phonons in the decay process. One notes, for example, the correspondence between a number of our theoretical curves and experimental results[14] obtained for the $MgO:Ni^{2+}$ spin system with $\sigma_2 > \sigma_1, \sigma_3$.

Admittedly, a model of a coupled spin-phonon system based on simple rate equations for the spin populations and phonon excitations (with the assumed linear phonon loss) is naive. Phenomena related to spatial variations within the sample,[8] coherence effects in the phonon system,[13] anisot-

ropy in the acoustic phonon characteristics, cross-relaxation and double-quantum effects, to name a few, have purposely been avoided. Nevertheless, a similar approach to the simpler two-level system has provided rather good qualitative and reasonable quantitative agreement in a number of physical systems. In addition, the existing data[7,10,14] on a number of $S=1$ systems (Fe^{2+} and Ni^{2+} in MgO) are not in opposition to our results; further data[15] to be published on the phonon characteristics in $MgO:Ni^{2+}$, such as phonon bandwidths and decays, also appear initially to be in reasonable accord with the simple model.

ACKNOWLEDGMENTS

A number of discussions with N. S. Gillis and D. Emin are gratefully acknowledged. Particular thanks are due J. P. Van Dyke for his considerable help with the numerical calculations.

---

*Work supported by the U. S. Atomic Energy Commission.

[1]J. H. Van Vleck, Phys. Rev. 59, 724 (1941).

[2]B. W. Faughnan and M. W. P. Strandberg, J. Phys. Chem. Solids 19, 155 (1961).

[3]P. L. Scott and C. D. Jeffries, Phys. Rev. 127, 32 (1962).

[4]J. A. Giordmaine and F. R. Nash, Phys. Rev. 138, A1510 (1965) and references cited therein.

[5]A. M. Stoneham, Proc. Phys. Soc. (London) 86, 1163 (1965).

[6]W. J. Brya and P. E. Wagner, Phys. Rev. Letters 14, 431 (1965); Phys. Rev. 157, 400 (1967).

[7]N. S. Shiren, Phys. Rev. Letters 17, 958 (1966).

[8]R. I. Joseph, D. H. K. Liu, and P. E. Wagner, Phys. Rev. Letters 21, 1679 (1968).

[9]C. H. Anderson and E. S. Sabisky, Phys. Rev. Letters 21, 987 (1968).

[10]W. J. Brya, S. Geschwind, and G. E. Devlin, Phys. Rev. Letters 21, 1800 (1968).

[11]S. A. Al'tshuler, R. M. Valishev, and A. Kh. Khasanov, Zh. Eksperim. i Teor. Fiz. Pis'ma v Redaktsiyu 10, 179 (1969) [Soviet Phys. JETP Letters 10, 113 (1969)].

[12]S. S. Rifman and P. E. Wagner, Solid State Commun. 7, 453 (1969).

[13]W. B. Mims and D. R. Taylor, Phys. Rev. Letters 22, 1430 (1969).

[14]N. S. Shiren, in *Proceedings of the Fourteenth Colloque Ampere, Ljubljana*, 1966 (North-Holland, Amsterdam, 1967).

[15]W. J. Brya, S. Geschwind, and G. E. Devlin (unpublished).

[16]We do not consider the effects of double-quantum transitions involving photons and/or phonons.

[17]Our results are very similar to those of Ref. 2, although the authors do not consider the early-time behavior in detail.

[18]A. G. Redfield, Phys. Rev. 98, 1787 (1955).

[19]E. Hahn, Phys. Rev. 80, 580 (1950).

[20]We have not detected the presence of a rate λ_3 in our solutions; however, from the form of λ_3, we surmise that it represents a characteristic internal equilibration rate for the spin transitions.

[21]An experiment performed just off line center, where our theories are not directly applicable, might show evidence for this behavior in the ΔN_{ij} transitions.

[22]The low peak value of Y_2 does not signify nonsaturation of the ω_2 transitions; the equalization of the ω_1 transitions with the associated increase in Y_1 also aids in the saturation of the ω_2 splittings. One therefore generates fewer ω_2 phonons as the outermost level populations are equalized.

[23]The system behavior for intermediate regions of the resonance is expected to lie between the extremes presented here.

[24]S. R. P. Smith, F. Dravnieks, and J. E. Wertz, Phys. Rev. 178, 471 (1969).

[25]V. W. Hughes and J. S. Geiger, Phys. Rev. 99, 1842 (1955).

[26]R. Le Naour, Phys. Rev. B 1, 2007 (1970).